Journal of Thermal Analysis and Calorimetry, Vol. 91 (2008) 2, 633–639

A KINETIC STUDY ON THE THERMAL BEHAVIOUR OF CHITOSAN

F. A. López[1], *A. L. R. Mercê*[2*], *F. J. Alguacil*[1] *and A. López-Delgado*[1]

[1]Departamento de Metalurgia Primaria y Reciclado, Centro Nacional de Investigaciones Metalúrgicas (CENIM), CSIC Avda. Gregorio del Amo 8, 28040 Madrid, Spain
[2]Universidade Federal do Paraná, Centro Politécnico, Departamento de Química, Laboratório de Equilíbrio Químico, CP 19081 Idj. das Américas, CEP 81531-990, Curitiba-PR, Brasil

The thermal behaviour of chitosan was studied by means of thermogravimetry, mass spectrometry and infrared spectrometry. Kinetic parameters were obtained by advanced kinetic evaluation (differential isoconversional analysis) from DSC curves, in non-isothermal conditions, at several heating rates, between 5 and 30°C min^{-1}. The results showed that the decomposition of chitosan does not follow a single mechanism because both the activation energy and the pre-exponential factor are not constant during the course of the reaction. A comparison with the results obtained by applying different conventional calculating methods is also shown.

Keywords: *chitosan, isoconversional analysis, kinetic, thermal degradation*

Introduction

Chitosan (poly-β(1→4)-2-amino-2-deoxy-*D*-glucopyranose) is a high molecular mass biopolymer which is obtained in alkaline media by the complete deacetylation of chitin [poly-β(1→4)-2-acetamide-2-deoxy-*D*-glucopyranose]. When deacetylation is incomplete a mixture of acetamide-polymer and amino-polymer are obtained producing materials with different properties called chitosans. Degrees of deacetilation of 70–80% are very common. The degree of deacetylation and the crystallinity of chitosans are the principal characteristics affecting both solubility in aqueous medium and capacity for forming complexes [1]. One of the major applications of chitosans is based on its ability to strongly coordinate metal ions, due to: 1) high hydrophilicity given the great number of hydroxyl groups it possesses, 2) a large number of chemically active amino groups and 3) a flexible structure of polymer chains that makes it compatible with the adsorption of metal ions. These characteristics, along with its broad and easy acquisition from natural and renewable sources allow a huge scope of applications related to environment [2], i.e. depuration of wastewaters [3, 4] and removing and recovery of metallic ions from industrial effluent [5–8].

Thermal analysis and kinetic studies are widely used for the characterization of polymeric materials and for the determination of reaction mechanism [9–11]. In the case of chitosan, several studies concerning the thermal degradation by means of TG, DTA and DSC techniques were reported and different kinetic values were obtained depending on the experimental conditions in which essays were performed [12–18].

The aim of this paper is to make comparison between the kinetic parameters of thermal degradation of chitosan, obtained by advanced kinetic evaluation (differential isoconversional analysis) from DSC curves and those calculated by several conventional methods in which a reaction order is assumed. The knowledge of thermal degradation kinetic may help a better understanding and planning of processes to recover metals or metal oxides previously absorbed on chitosan.

Experimental

Sample characterization

A commercial sample of chitosan (75% degree of deacetylation, Sigma-Aldrich, USA) was used in this study.

Infrared spectrometry (FTIR, Nicolet Magna 750), thermogravimetric analysis (Shimadzu TGA 50H), mass spectrometry (QMS-200 Balzers Omnistar) were used for sample characterization.

FTIR spectrum was recorded in the wavenumber range between 3500–500 cm^{-1}, resolution of 4 cm^{-1} and 32-times scanning. Discs of 1 cm of diameter were prepared by mixing chitosan with CsI (1:500 mass/mass%) using a 15 tonnes hydraulic press.

TG curve was recorded at a heating rate of 5°C min^{-1}, from room temperature up to 600 °C, in argon atmosphere (20 ml min^{-1}). Around 10 mg of sample and alumina crucibles were used in the test. The

---

* Author for correspondence: flopez@cenim.csic.es

1388–6150/$20.00
© 2007 Akadémiai Kiadó, Budapest

Akadémiai Kiadó, Budapest, Hungary
Springer, Dordrecht, The Netherlands

outlet of the TG was connected, through a capillary tube held at 200°C to the mass spectrometer. In such a configuration, evolved gas products by the thermal treatment could be simultaneosly analyzed by quadrupolar mass spectroscopy (QMS). The ion detection was performed through secondary electron multiplier which detects very low pressures within Channeltron detector. A mass range between 40 and 130 atomic mass unit was studied.

Sealed aluminium crucibles (isochoric conditions) were used for DSC studies (Shimadzu DSC-50) and the same experimental conditions as those used for TG analysis.

Determination of kinetics parameters

The kinetic of the thermal behaviour of chitosan was studied by DSC in non-isothermal conditions. Curves were obtained at several heating rates, between 5 and 30°C min^{-1}. Kinetic parameters were evaluated by isoconversional method which involves determination of temperatures corresponding to a certain, arbitrarily chosen values of the conversion extent α recorded in the experiments carried out at different heating rates β. Commonly applied isoconversional methods are known as methods of Flyn and Wall [11], Ozawa [19, 20] and Friedman [21].

The model-free method was used for the calculation of kinetic parameters by means of simulations with the AKTS-Thermokinetics software [22, 23], after baseline subtraction and normalization of exothermal peak obtained for different heating rates.

Results and disccusion

Figure 1 shows the FTIR spectrum of chitosan. The most probable assignation of the absorption bands is given in Table 2. Bands appearing at 1646, 1096 and 1590 cm^{-1} corresponded to the $\nu_{C=O}$, $\nu_{C–O}$ stretching and δ_{NH_2} bending modes, respectively. These bands indicate that chitosan is not completely deacetylated [24, 25].

Table 1 Forms of the *f*(α) function according to the reaction model and their commonly used abbreviations

Autocatalytic:$(1–\alpha)^n\alpha^m$	An:$n(1–\alpha)\ [–\ln(1–\alpha)]^{(1–1/n)}$
	A1.5:$1.5(1–\alpha)\ [–\ln(1–\alpha)]^{(1/3)}$
	A2:$2(1–\alpha)\ [–\ln(1–\alpha)]^{(1/2)}$
Fn:$(1–\alpha)^n$	
F1:$1–\alpha$	Rn:$n(1–\alpha)^{(1–1/n)}$
F2:$(1–\alpha)^2$	R2:$2(1–\alpha)^{(1/2)}$
F3:$(1–\alpha)^3$	R3:$3(1–\alpha)^{(2/3)}$
Pn:$n\alpha^{(1–1/n)}$	D1:$1/(2\alpha)$
P2:$2\alpha^{(1/2)}$	D2:$[–\ln(1–\alpha)]^{-1}$
P3:$3\alpha^{(2/3)}$	D3:$1.5\ [1–(1–\alpha)(1/3)]^{-1}(1–\alpha)^{(2/3)}$
P4:$4\alpha^{(3/4)}$	D4:$1.5\ [(1–\alpha)^{(–1/3)}–1]^{-1}$

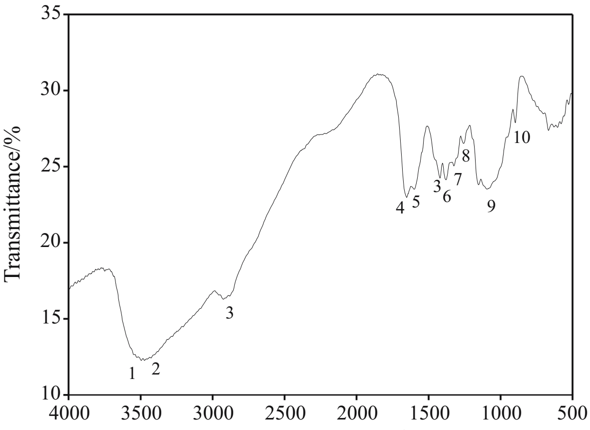

Fig. 1 FTIR spectrum of chitosan

Figure 2 shows TG and DSC curves of chitosan. A first endothermic peak is observed between 42–125°C, with a minimum T_{peak} at 81°C. A mass loss of 9.2% is associated to this effect and it is attributed to the evaporation of absorbed water in the inner polymer. A second effect is observed between 268–312°C with an exothermic peak at 292°C. This effect is also associated to a mass loss (51.2%) which corresponded to the thermal degradation of polymeric chain with vaporization of volatic compounds. The pyrolysis of polysaccharides structure starts by a random split of the glycosidic bonds, followed by a further decomposition forming acetic and butyric acids and a series of lower fatty acids, where C2, C3 and C6 predominate [13–15]. The energy associated to this second effect is 212.3 J g^{-1}. Finally a

Table 2 Assignation of FTIR absorption bands of chitosan

Wavenumber/cm^{-1}	Identification of absorption bands
3496 (1)	OH group (ν_{OH})
3345 (2)	NH group-stretching vibration (ν_{NH})
2926, 2873, 1421, 1322, 1249 (3)	symmetric or asymmetric CH_2 stretching vibration attributed to pyranose ring (ν_{CH})
1646 (4)	C=O in amide groups (amide I band)
1593 (5)	NH_2 bending vibration in amino group (δ_{NH_2})
1421,1322 (6)	vibrations of OH, CH in the ring
1381 (7)	CH_3 in amide group
1249 (8)	C–O group
1156 (9)	–C–O–C– in glycosidic linkage
1096, 1030 (10)	C–O group ($\nu_{C–O}$) in amide group
897 (11)	CH_3COH group

(number in bracket indicates the corresponding band in Fig. 1)

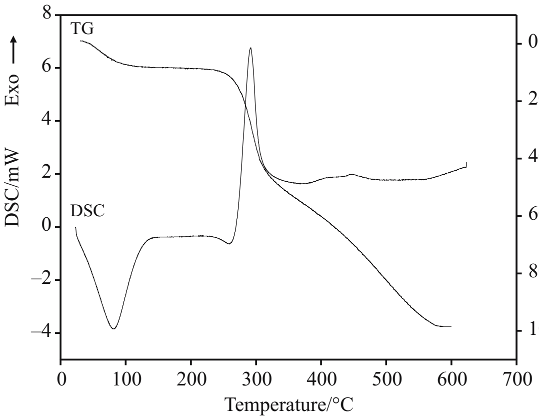

Fig. 2 TG and DSC curves of chitosan (heating rate, 5°C min^{-1})

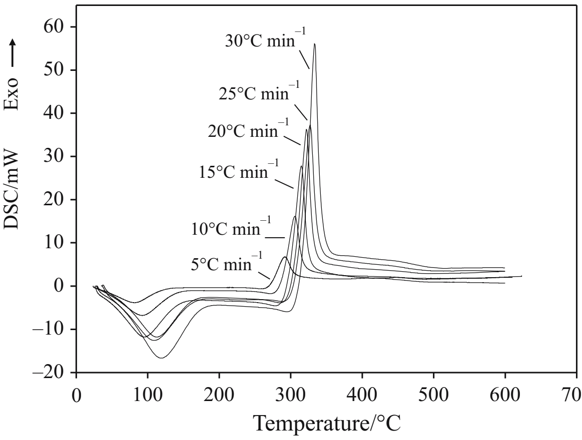

Fig. 3 DSC curves at different heating rates

third effect (exothermic) can be observed between 387–471°C, which corresponds to the residual cross-linked degradation of chitosan. The mass loss associated to this effect is 38.9%.

Figure 3 shows the DSC curves for different heating rates (5–30°C min^{-1}). Data in Table 3 show the variation of peak temperature and energy, corresponding to both the endothermic and first exothermic effect, as a function of the heating rate. For both effects, peak temperature increases and energy (absolute value) decreases as heating rate increases. An anomalous value of energy is observed at 30°C min^{-1}, in the case of the endothermic effect. Probable, it is due to the very high heating rate. Data for the third effect were not included because they were only observed at the lowest heating rate, this 5°C min^{-1}. For higher rate, this effect is not observed. Kinetic parameters of thermal degradation of chitosan were calculated in the base of the first exothermic effect because in this range of temperature the breaking down of polymeric chain takes place.

DSC signals, after correction of the baseline, were used for the estimation of the reaction progress. The ob-

Table 3 DSC data of chitosan vs. heating rate

β/ °C min^{-1}	Peak 1 endothermic effect				Peak 2 exothermic effect			
	T_0/°C	T_e/°C	T_p/°C	ΔH/J g^{-1}	T_0/°C	T_e/°C	T_p/°C	ΔH/J g^{-1}
5	41.6	125.3	81.3	–179.8	268.4	311.6	291.8	212.3
10	45.1	138.5	92.2	–209.8	280.1	325.6	305.8	185.5
15	73.2	134.3	94.9	–76.8	292.2	332.6	314.8	197.8
20	89.3	152.8	112.5	–69.7	299.5	339.0	322.1	173.3
25	84.8	151.5	109.0	–60.1	303.2	346.1	327.1	146.2
30	83.3	168.6	119.2	–122.7	308.0	354.4	333.3	189.2

Table 4 Activation energy and pre-exponential factor for the thermal decomposition of chitosan calculated from DSC, by assuming commonly applied simplified reaction models

Models	E/kJ mol^{-1}	A/s^{-1}	n	m
Autocatalytic: $(1–\alpha)^n\alpha^m$	152.26	2.13 10^{12}	1.48	0.552
An:$n(1–\alpha)[–\ln(1–\alpha)]^{(1–1/n)}$	111.55	1.3 10^8	1.39	–
A1.5:1.5 $(1–\alpha)[–\ln(1–x)]^{(1/3)}$	102.02	1.69 10^7	1.5	–
A2:$2(1–\alpha)[–\ln(1–\alpha)]^{(1/2)}$	72.37	2.84 10^4	2	–
Rn:$n(1–\alpha)^{(1–1/n)}$	210.49	–8.15 10^{16}	– 2.64	–
R2:$2(1–\alpha)^{(1/2)}$	96.38	1.96 10^6	2	–
R3:$3(1–\alpha)^{(2/3)}$	154.78	1.42 10^8	3	–
F1:1–α	161.31	5.06 10^{12}	1	–
F2:$(1–\alpha)^2$	291.17	8.46 10^{24}	2	–
ASTM E698	127.90	4.82	–	–

tained α–T values were applied for the calculation of the E and A kinetic parameters either by isoconversional method of Friedman or by simplified methods with the function $f(\alpha)$ being arbitrarily assumed to be in the form of the equation described in Table 1. Additionally, kinetic parameters were calculated by the ASTM E698 [26] method. Activation energy values obtained by these simplified methods are presented in Table 4. It can be observed the variability of values obtained for activation energy and pre-exponential factor depending on the model used for calculation.

DSC signals, corresponding to the first exothermic effect, are presented in Fig. 4. Heating rates (in °C min^{-1}) are marked on the curves. Experimental results, after normalization and subtraction of base-lines are drawn in plots by symbols, and prediction of the reaction rates by solid lines. The Fig. 5 depicts the results of the Friedman analysis. The conversion rates, $d\alpha/dt$, measured at different extents of the temperature at different heating rates (straight lines on the diagrams) allowed determination of the kinetic parameters A and E for the reaction as a function of the reaction progress, which can be observed in Fig. 6.

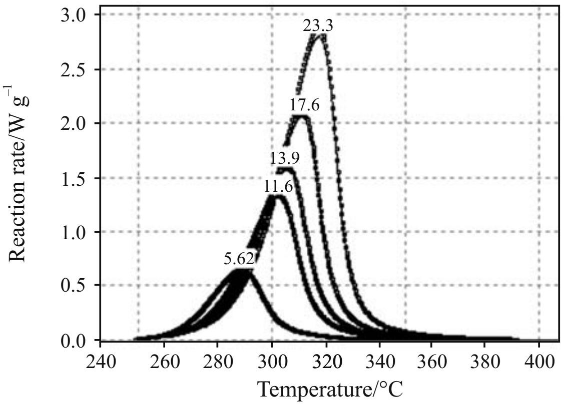

Fig. 4 Advanced kinetic description of normalized non-isothermal DSC-signal as a function of the time for the decomposition of chitosan (Experimental data are represented as symbol, solid lines represent the calculated signals. The values of the heating rate in °C min^{-1} are marked on the curves)

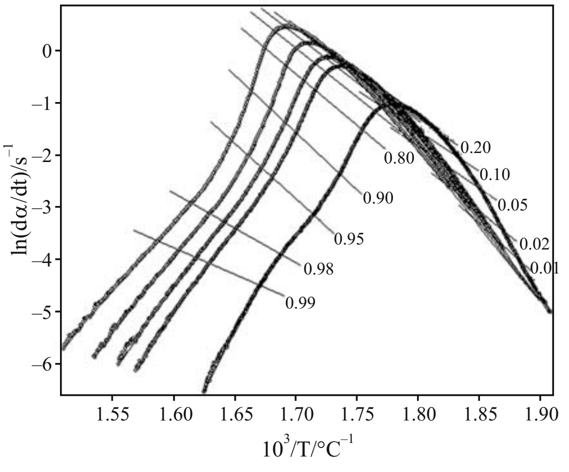

Fig. 5 Friedman analysis for the decomposition of chitosan

The results presented in Fig. 6 show that the decomposition of chitosan does not follow a single mechanism because the values of the activation energy and pre-exponential factor are not constant during the course of the reaction. Clearly visible is the dependence of the kinetic parameters on the reaction extent. This observation indicates that the decomposition of chitosan is a complex reaction which cannot be described in terms of a single pair of Arrhenius parameters and commonly used set of reaction models.

The activation energy ranges between 185.7 and 95.6 kJ mol^{-1} along of the reaction course ($0<\alpha<1$) and the pre-exponential factor varies between $2.37\cdot10^{14}$ and $2.45\cdot10^{6}$ s^{-1}. For a conversion degree of $0.1<\alpha<0.9$, values range between 183.9 and 142.6 kJ mol^{-1} were obtained for the activation energy and between $4.49\cdot10^{14}$ and $3.80\cdot10^{9}$ s^{-1}, for the pre-exponential factor. The activation energy calculated by ASTM E698, was 127.9 kJ mol^{-1} and the pre-exponential factor, 4.82 s^{-1}.

Literature reports different values depending on the calculation method used. Qu *et al.* [16], applying the method proposed by Broido [27], reported an E_a value of 113.14 kJ mol^{-1} for a 88% deacetylated chitosan. Results were obtained from TG curves recorded at different heating rates in an inert atmosphere.

De Britto *et al.* [17], also from TG curves and in an inert atmosphere, reported an E_a value of 82.1 kJ mol^{-1} by applying the method of Briodo [27] in non-isothermal conditions. In the case of isothermal conditions and by the application of MacCallum's equations [28], E_a

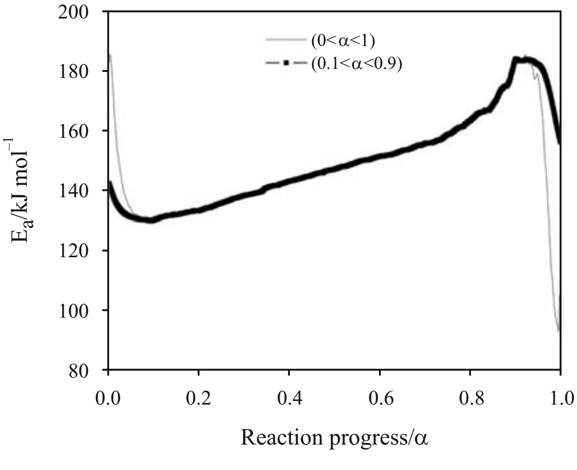

Fig. 6 Activation energy (E_a) and pre-exponential factor (A) determined by Friedman analysis as a function of the reaction progress for the decomposition of chitosan

ranged between 137.9 and 157.0 kJ mol^{-1} for $0.05<\alpha>0.19$ were obtained. These results were based on the assumption of constant activation energy during the reaction course.

Recently, Wanjun *et al.* [18] determined the apparent activation energy for the thermal degradation of chitin and chitosan from TG curves using the Friedman's method (model free iso-conversional method) [21]. Values of E_a ranging between 150 and 300 kJ mol^{-1} were obtained depending on the conversion degree. By the application of DAEM (Distributed Activation Energy Model) [29], 189 kJ mol^{-1} (standard deviation 34 kJ mol^{-1}) and $1.01\cdot10^{15}$ s^{-1} were the values obtained for E_a and A respectively.

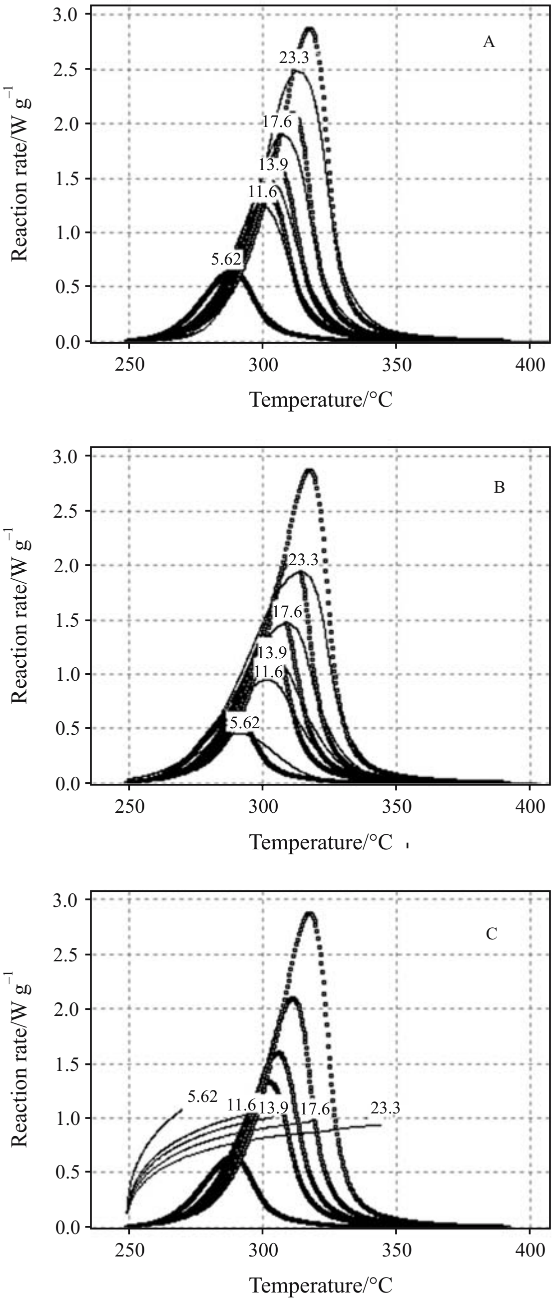

Fig. 7 Simplified kinetic description of normalized non-isothermal DSC-signal as a function of the temperature for the decomposition of chitosan at five heating rates. A – autocatalytic, B – Fn-th order reaction, C – Pn order reaction. (Experimental data are represented as symbols, solid lines represent the calculated signals. The values of heating rates in °C min^{-1} are marked on the curves)

The criteria employed by Wanjun *et al.* [18] are similar to those used in this work. Those authors assume the pre-exponential factor is constant and so a unique value of E_a is obtained. But A is, in this case, strongly depending on the conversion degree (Fig. 6).

The application of the simplified kinetics (arbitrary assumption of the reaction mechanism) does not allow the correct simulation of the experimental results. Figure 7 presents the trials of the simulation of the experimental decomposition course of chitosan by applying the simplified models assuming: autocatalytic reaction model (A), Fn-th reaction model (B) and Pn reaction model (C). The results presented in Fig. 7 indicate that the commonly used method of the prediction of the reaction rates based on the assumption of the constancy of the reaction mechanism cannot lead to the proper description of the process.

Thermal degradation of chitosan is a complex reaction. Different decomposition products were observed by mass spectrometry during the thermal treatment. Mass fragment signals of up to *m*/*e*=130 amu were recorded. The mass fragments corresponding to gases evolved during the thermal degradation of chitosan and ranged between 40 and 90 amu are presented in Fig. 8. At the beginning of the decomposition reaction (Fig. 8A) mass fragments of *m*/*e* 43, 44, 45, 46 and 80 amu are observed. Mass fragment of 44 amu being of very high intensity. As temperature increases (Fig. 8B) intensities of signals corresponding to 42, 43, 44, 45, 46 and 80 highly increase. New signals corresponding to m/e 50, 51, 52, 53, 54, 55, 56, 57, 58, 68, 69, 78, 79, 81 and 82 appeared at this temperature.

At 400°C (Fig. 8C) a general decreasing of signals is observed, those corresponding to *m*/*e* 50 and 58 amu, especially. The mass fragments of *m*/*e* 46, 79 and 82 amu are not observed at this temperature. Finally, at 600°C (Fig. 8D), the mass fragments of *m*/*e* 43, 44 and 80 amu are observed.

Hayes and Davies [30] suggested that fragments are derived from the monomer units I and II by breaking of the p-glycoside bond between monomer units (monomer I and monomer II).

The mass spectrum obtained at 300°C (Fig. 8B) is similar to that reported by Mattai and Hayes [31]. The principal compounds indentified are: acetic acid ($C_2H_4O_2$) (*m*/*e*=43, 45, 60), acetic anhydride (C_2H_2O) (*m*/*e*=42),(C_2H_4N)$^+$ (*m*/*e*=42), acetamide (C_2H_5NO) (*m*/*e*=59), pyrrol (C_4H_5N) and 2-butenol (C_4H_7O)

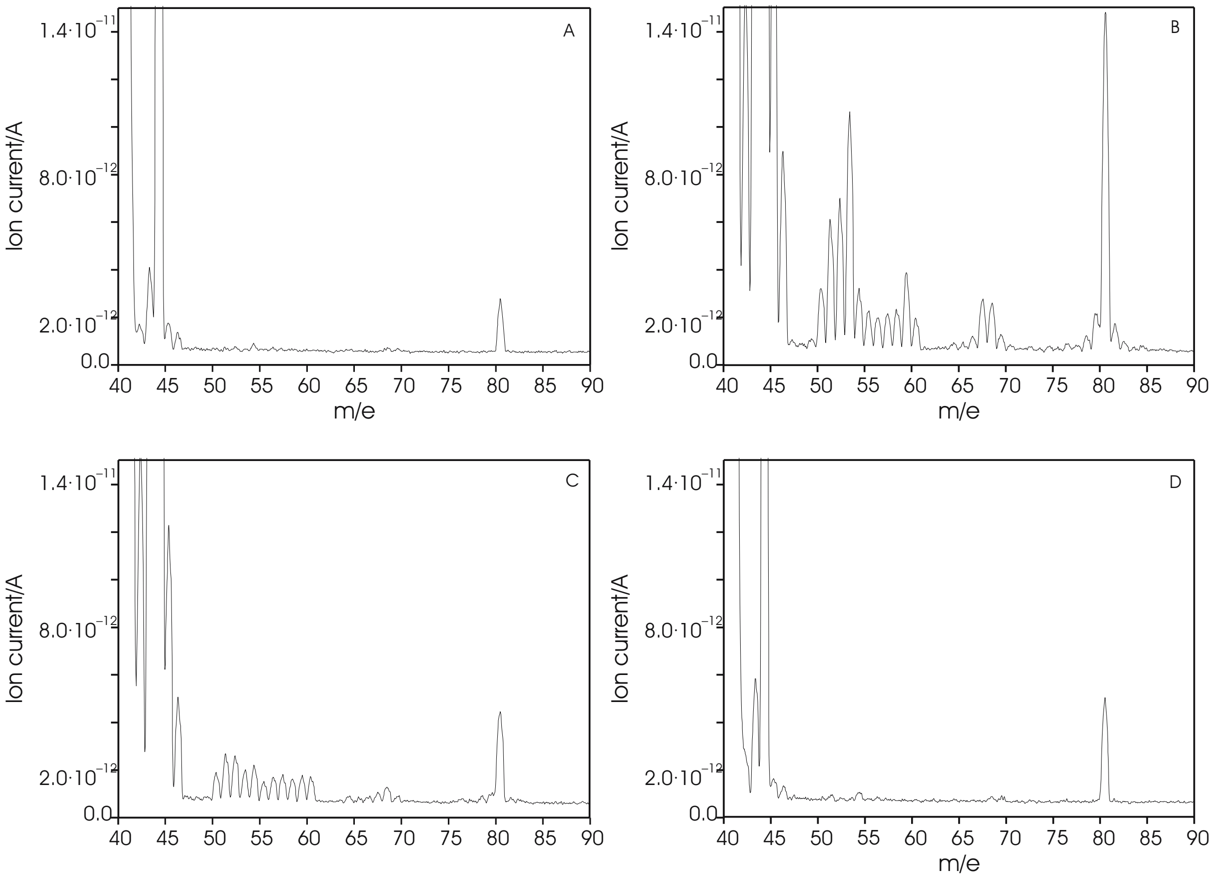

Fig. 8 Mass spectra of gases evolved during the thermal treatment of chitosan at different temperatures (A – 260; B – 300; C – 400; D – 500°C)

(*m*/*e*=70). Other signals of less intensity correspond to acetone (C_3H_6O) (*m*/*e*=58), trimethylamine (C_3H_9N) (*m*/*e*=83) and 1-methylpyrrole (*m*/*e*=81). Peaks of *m*/*e* 67 ($C_5H_7^-$) and 80 ($C_5H_6N^+$) are reported being of high intensity for chitosan and of low intensity for chitin and N-acetyl-*D*-glucosamine, this strongly indicating that these fragments originate from monomer I. The peak at *m*/*e* 60 was determined to be $C_2H_4O_2$ and this peak was found to be identical in the spectra of N-acetyl-*D*-glucosamine and chitin, indicating that this fragment originates from monomer II.

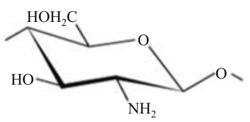

I

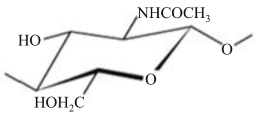

II

Acetic acid (*m*/*e* 60) is a characteristic product of the pyrolysis of chitin and N-acetyl-*D*-glucosamine. The removal of a molecule of water from acetic acid could produce the peak at *m*/*e* 42. The peak at *m*/*e* 80 is C_5H_6N. The peak at *m*/*e* 67 is made up of two ions, C_4H_5N and C_5H_7.

Then it could be concluded that thermal decomposition of chitosan starts with the breaking down of the bond C–O–C. It implies the depolymerization of chitosan and the formation of monomers which carries out the formation of acetamide, C_2H_5NO, (*m*/*e*=59). These results fit well to those reported in the literature on temperature-programmed pyrolysis [32, 33].

Conclusions

Chitosan was characterized by FTIR and TG/DSC. Thermal degradation of chitosan occurs in three steps, but strictly from a point of view of the polymer decomposition, the exothermic effect occurring between 268–312°C is the most important one, because it is associated with the breaking down of the polymeric chain. Depolymerization through the formation of different monomers was studied by MS. Non-isothermal conditions were used for the study of thermal behaviour of chitosan by DSC. Kinetic parameters were calculated by isoconversional methods. The results have shown the decomposition of chitosan is a complex reaction, which cannot be described in terms of a single pair of Arrhenius parameters. Both the activation energy and the pre-exponential factor are strongly dependent on the conversion degree, with values ranging from 185.7 to 95.6 kJ mol^{-1} and from $2.37\cdot10^{14}$ to $2.45\cdot10^{6}$ s^{-1}, respectively, along the reaction course ($0<\alpha<1$).

References

1 E. Guibal, Sep. Purif. Technol., 38 (2005) 43.
2 S. Badel and T. A. Kuriawan, J. Hazard. Mater., 97 (2003) 219.
3 J. Roussy, P. Chastellan, M. van Vooren and E. Guibal, Water Res., 31 (2005) 369.
4 S. Babel and T. A. Kurniawan, Chemosphere, 54 (2004) 951.
5 A. P. Franco, J. Felcman, A. López-Delgado and A. L. R. Mercê, 29ª Reuniao Anual Sociedade Brasileira de Química. Sao Paulo-Br., 19–22 May 2006.
6 M. M. Jaworska and E. Guibal, Waste Manage., 23 (2003) 339.
7 L. Dambies, T. Vincent and E. Guibal, Water Res., 36 (2002) 3699.
8 M.S. Masri, F. W. Reuter and M. Friendman, J. Appl. Polym. Sci., 18 (1974) 675.
9 B. A. Howell, J. Therm. Anal. Cal., 85 (2006) 165.
10 J. M. Criado, L. A. Pérez-Maqueda, F. J. Gotor, J. Málek and N. Koga, J. Therm. Anal. Cal., 72 (2003) 901.
11 J. H. Flynn and L. A. Wall, J. Res. Nat. Bur. Standards, 70 A (1966) 487.
12 C. Peniches-Covas and M. S. Jiménez, Carbohidr. Polym., 9 (1988) 249.
13 J. M. Nieto, C. Peniche-Covas and G. Padrón, Thermochim. Acta, 176 (1991) 63.
14 G. Cárdenas, L. Bernal and L. H. Tagle, Thermochim. Acta., 195 (1992) 33.
15 C. G. T. Neto, J. A. Giacometti, A. E. Job, F. C. Ferreira, J. L. C. Fonseca and M. R. Pereira, Carbohydr. Polym., 62 (2005) 97.
16 X. Qu, A. Wirsén and A. C. Albertsson, Polymer, 41 (2000) 4841.
17 D. De Britto and S. P. Campana-Filho, Polymer Deg. Stab., 84 (2004) 353.
18 T. Wanjun, W. Cunxin and C. Donghua, Polym. Degrad. Stab., 87 (2005) 389.
19 T. Ozawa, Bull. Chem. Soc. Jpn., 38 (1965) 1881.
20 T. Ozawa, J. Thermal Anal., 2 (1970) 301.
21 H. L.Friedman, J. Polym. Sci., 6 (1964) 183.
22 B. Roduit, C Borgeat, B. Berger, P. Folly, B. Alonso, J. N. Aebischer and F. Stoessel, J. Therm. Anal. Cal., 80 (2005) 229.
23 Advanced Kinetics and Technology Solutions, (AKTS-Thermokinetics software and AKTS-Thermal Safety v.2.41) 2006.
24 G. Cardenas, P. Orlando and T. Edelio, Int. J. Biol. Macromol., 28 (2001) 167.
25 Z. Osman and A. K. Arof, Electrochim. Acta, 48 (2003) 993.
26 ASTM E698-99. Standard Test Method for Arrhenius Kinetic Constants for Thermally Unstable Materials. ASTM International. 10 Apr. 2001.
27 A. Broido, J. Polym. Sci. Part A-2 Polym. Phys., 7 (1969) 1761.
28 J. R. MacCallum, Comprehensive Polymer Science, Pergamon Press, Oxford 1989, p. 903.
29 K. Miura, Energy Fuel, 12 (1998) 864.
30 E. R. Hayes and D. H. Davies, In: R. A. A. Muzzarelli and R. A. Pariser, Eds, Proc. First International Conference on Chitin/Chitosan, MIT, Cambridge, MA (1978), p. 406.
31 J. Mattai and E. R. Hayes, J. Anal. Appl. Pyrol., 3 (1982) 327.
32 H. Sato, H. Ohtani, S. Tsuge, K. Aoi, A. Takasu and M. Okada, Macromolecules, 33 (2000) 357.
33 C. Jianhong, W. Mingfu and H. Chi-Tang, J. Agric. Food Chem., 46 (1998) 3207.

Received: January 22, 2007
Accepted: May 10, 2007
OnlineFirst: August 31, 2007

DOI: 10.1007/s10973-007-8321-3